UNDERSTANDING THE ROLE OF TRANSGENIC CATALASE IN T-CELL
DEVELOPMENT IN MURINE-BASED STUDIES

by

Richard M. Smith

A Thesis Submitted to the Faculty of

The Harriet L. Wilkes Honors College

in Partial Fulfillment of the Requirements for the Degree of

Bachelors of Arts in Honors Liberal Arts and Sciences

with a Concentration in Biological Chemistry

Wilkes Honors College of

Florida Atlantic University

Jupiter, Florida

May 2012

UNDERSTANDING THE ROLE OF TRANSGENIC CATALASE IN T-CELL DEVELOPMENT IN MURINE-BASED STUDIES

by

Richard M. Smith

This thesis was prepared under the direction of the candidate's thesis advisor, Dr. Paul Kirchman, and has been approved by the members of his supervisory committee. It was submitted to the faculty of The Honors College and was accepted in partial fulfillment of the requirements for the degree of Bachelor of Arts in Honors Liberal Arts and Sciences.

SUPERVISORY COMMITTEE:

_____   _____

Dr. Paul Kirchman   Dr. Ann Griffith

_____   _____

Dr. Michelle Ivey   Dr. Howard Petrie

_____

Dean Jeffrey Buller, Wilkes Honors College

_____

Date

ACKNOWLEDGEMENTS

ABSTRACT

Author: Richard M. Smith

Title: Understanding the Role of Transgenic Catalase in T-Cell Development in Murine-based Studies

Institution: Wilkes Honors College of Florida Atlantic University

Thesis Advisors: Dr. Ann Griffith and Dr. Paul Kirchman

Degree: Bachelors of Arts in Honors Liberal Arts and Sciences

Concentration: Biological Chemistry

Year: 2012

The thymus provides a unique microenvironment that facilitates T lymphocytes differentiation and maturation. However, the thymus atrophies after puberty which leads to an overall decline in immune capacity. Previous microarray data revealed high expression of metabolism gene pathways and low gene expression of certain peroxide scavenger enzymes such as catalase in thymic stromal compartments. From this data, we postulate that thymic stromal cells are highly susceptible to oxidative damage. We utilized a transgenic mice model overexpressing human catalase targeted to the mitochondria (mCat) to test our hypothesis that greater oxidative protection should lower the degree of thymus atrophy. Our experiment focused on a direct comparison of organ weights (thymus, kidney, lymph nodes, spleen and heart), cellularity and histology between transgenic and wildtype mice. We found that mCat mice had selective increases in thymus size.

DEDICATION

To my Mom and Big Sis

TABLE OF CONTENTS

LIST OF TABLES

LIST OF FIGURES

INTRODUCTION

Cellular and organ components of the immune system equip the body with vital defensive capabilities against pathogenic diseases and infections. The immune system provides non-specific and specific protection through a wide variety of components including lymphocytes, macrophages, granulocytes, dendritic cells, lymph nodes, spleen, thymus and other important components. Cellular components of the immune system are able to elicit innate or an adaptive responses to pathogens. Innate responses are present at birth and prompt non-specific reactions; these innate responses are usually initiated by phagocytic cells such as macrophages and granulocytes in a general response to foreign antigens (Janeway, 1999). On the other hand, adaptive immune responses are specific to particular infections and confers protective long-term immunity (Janeway, 1999).

There is some overlap between innate (non-specific) and adaptive (specific) immune responses, but most importantly, all cellular agents must work together to have a fully functioning immune system. Nonetheless, T lymphocytes (T cells) and B lymphocytes (B cells) are two of the major mediators of cellular immunity. T and B lymphocytes facilitate adaptive responses as either humoral immunity (antibody mediated) responses by B cells, or cell-mediated immunity by T cells (Kuby, 1997). Both sets of cells originate from multipotent progenitor cells (hematopoietic stem cells or HSCs) that originate in the bone marrow (Janeway, 1999). Both lymphoid cell lineages, as well as all other classes of immunocompetent cells, are sometimes lost through cellular senescence, selective apoptosis, and bleeding (Prockop et al., 2002). Therefore, the body needs a specific site or organ to replenish lost lymphocytes to maintain homeostasis. B-

cell progenitors differentiate and mature in the bone marrow. Although T cell progenitors originate in the bone marrow, they circulate in the blood stream and exit to the thymus for differentiation by various intrathymic signals such as chemokines, Kit ligands and Notch ligands (Petrie & Zuniga-Pflucker, 2007). Therefore, the thymus is a major lymphoid organ which facilitates T-lymphocyte differentiation, maturation, and replenishment of naïve T-cells.

The thymus is a bi-lobed organ (in comparison to peripheral lymphoid organs such as lymph nodes), and is located in the upper chest cavity superior and proximal to the heart (Janeway, 1999). In human thymuses, each lobe consists of several lobules, or grape-like clusters; each lobe is separated by a capsule but adjoined to each other by connective tissue. Moreover, each lobe has two distinct compartments: an outer cortex that contains a majority of immature T cells and an interior medulla with fewer lymphocytes (Kuby, 1997). In contrast to human thymus anatomy, thymuses in young mice do not contain distinctive lobules; rather, several medullary islets are present. Furthermore, researchers are greatly inclined to study murine, or mice-based models in immune research because of their comparative anatomy with humans, mice models are readily available, and these modeled studies avoid greater ethical dilemmas presented by human-based studies.

Even though the thymus is compartmentalized into cortical and medullary regions, the structural frame for the thymus is a matrix of epithelial and mesenchymal stromal cells which also consists of dendritic cells, macrophages and other lymphocytes (Kuby, 1997; Petrie & Zuniga-Pflucker, 2007). Consequently, there are both cortical and medullary stromal cells that provide a unique intra-thymic environment for transient, differentiating lymphocytes. Several studies assert that the stromal compartment is responsible for the homing signals that the HSCs receive to migrate to the thymus and adopt T-lineages (Griffith et al., 2012; Kuby, 1997; Petrie, 2002). Thus, the thymic stromal region is very important in facilitating lymphocyte development and adaptive immunity responses.

Thymic homing progenitors (THPs) are a subset of HSCs from the bone marrow that are recruited to the thymus. Following their extravasation from the blood stream, these THPs enter the thymus through relatively large (high endothelial venules) blood vessels adjacent to the medulla at the perimedullary cortex junction (Petrie & Zuniga-Pflucker, 2007). Researchers estimate that approximately 10-100 cells enter the thymus of young adult mice each day, but the thymus can actively recruit progenitors on a need basis (Petrie, 2002). Thymocyte differentiation occurs in several distinct phases (Fig. 1) which depend on changes in receptor gene expression (example, α:β or γ:δ receptor gene rearrangement), the presence of cell surface markers, and expression of T cell receptors such as the CD4 and CD8 co-receptors (Janeway, 1999).

3
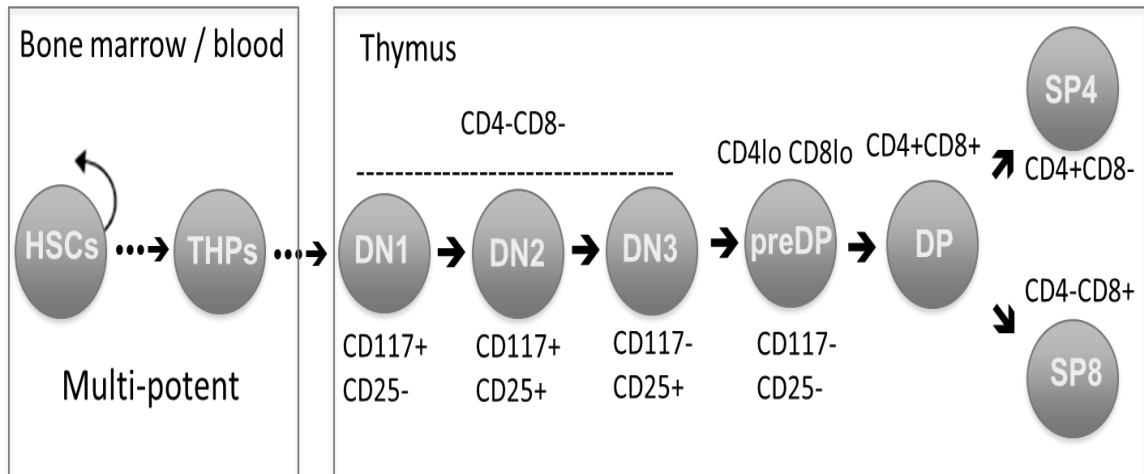
Figure 1. Post-natal T-cell differentiation. (Credit: Jianjun Shi, Scripps-Florida)

At the early stages of T cell differentiation, the cells are classified as double negative because they do not present either markers for CD4 or CD8 (CD4-CD8 -/-). Over the course of T-lymphocyte maturation, double negative subtypes (DN1-DN3) develop into pre-double positive (pre-DP), then CD4+CD8+ double positives (DP) further mature into either CD4+CD8- or CD4-CD8+ single positive (SP) T cells (Cruse & Lewis, 1999). The overall migration of differentiating thymocytes follows a U-shaped pattern (reviewed in Petrie, 2007). From the time that thymocytes enter the thymus at the corticomedullary junction, they move outwards towards the subcapsular region of the cortex as DN cells, and then move inwards as DP and SP cells back to the medulla before exiting the thymus (SP cells only) into the bloodstream and from then on some may enter the lymphatic circulation towards secondary lymphoid organs such as lymph nodes (Petrie & Zuniga-Pflucker, 2007).

Between DN1 and pre-DP stages, lymphocyte progenitors undergo rapid proliferation especially in the transition between DN3-preDP subtypes. Often this proliferative activity is an observed million fold expansion in cell numbers as the original 10-100 THPs increase to approximately 5×10^7 cells (Janeway, 1999; Petrie, 2002). At the DN3 stages, cells undergo at least one T cell receptor β (TCRβ) allele rearrangement which permanently commits the cells to T lineage (Petrie & Zuniga-Pflucker, 2007). Cells with rearranged TCRβ rearrangements are allowed to proliferate while defective thymocytes undergo apoptosis, or programmed cell death.

As thymocytes transition to the DP stage, thymocyte proliferative capacity plateaus and is greatly inhibited (Petrie & Zuniga-Pflucker, 2007). During this process, cells undergo positive (clonal) selection. Throughout positive selection, surviving DP cells are selected for their ability to recognize self-major histocompatability complex (MHC) molecules and other self-antigens. At this stage, recognizing self is favorable and indicates that cells have indeed adopted T lineage potentials. Therefore, cells that pass the positive selection process are able to interact with both self and foreign antigens (Cruse & Lewis, 1999). Later, post-positive selected thymocytes move towards the medulla where they encounter dendritic cells that facilitate negative clonal deletion (Petrie & Zuniga-Pflucker, 2007). Dendritic cells help to present thymocytes with non-thymic tissue restricted antigens (TRAs); for example, dendritic cells present ectopic eye, lung or other tissue antigens to thymocytes; however, auto-reactive responses to ectopic tissue elicit clonal deletion (apoptosis) or clonal anergy (cell inactivation) of potentially self-reactive thymocytes (Cruse & Lewis, 1999; Petrie & Zuniga-Pflucker, 2007). On a whole, only

5

3% of all proliferated thymocytes survive negative selection (Janeway, 1999). At the SP stage, some thymocytes are not fully mature and undergo further "training" in recognizing self-antigens until they develop a form of self-tolerance before exiting the thymic environment deep in the medulla as naïve T cells (Petrie & Zuniga-Pflucker, 2007).

The overall length of stay in the thymus for thymocytes averages from 21-28 days (Petrie & Zuniga-Pflucker, 2007). T lymphocyte differentiation results in several T lineages that depend on various cell surface markers or receptors that each lymphocyte subset presents. These lineages include CD4 (T-helper, T_H), CD8 (cytotoxic T-cells, T_C), Natural Killer T cells (NKT), and others. However, there is little evidence that suggest that cells other than CD4, CD8, or $\gamma\delta$ T cells (less than 5%) mature in the thymus (Cruse & Lewis, 1999; Petrie, 2002). The two most well defined subpopulations of T cells are CD4 (T-helper, T_H) and CD8 (cytotoxic T-cells, T_C). CD4 cells recognize antigens via MHC class II receptors and release cytokines to attract B cells, T_C cells, and other phagocytic cells. On the other hand, CD8 cells utilize MHC class I receptors to interact with antigens and are able to perform cytotoxic activity, thereby killing pathogenic cells and altered self-cells such as tumor cells (Kuby, 1997). A healthy thymus supports a continuous output of new T cells. Nevertheless, there is progressive thymus atrophy, especially after puberty, which greatly reduces the number of naïve T cells produced by the thymus. In mice and other rodents, the size of the thymus becomes physically smaller (Fig. 2); however, in humans, the size stays relatively the same after puberty, but the t-cell output drops as adipose tissue fills the lymphoid space over time (Haynes et al.,

2000). Therefore, researchers observe a pattern wherein the production new T cells is proportional to thymic mass (Griffith et al., 2012). Thus, lower T cell output greatly reduces the body's ability to fight new diseases and pathogens.
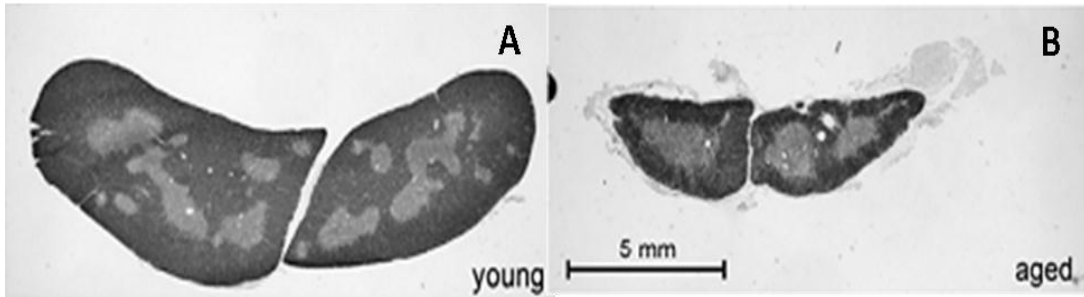
Figure 2. Thymic atrophy in mice. Transverse thymus sections showing darker stained cortex and smaller (lighter stained) medullary islets in mice. (A) Thymus of young mice at 4-5 weeks old. (B) Aged mice are sacrificed at 12 months old. Note the smaller size aged thymus with few to no distinct medullary islets. (Griffith et al., 2012)

The mechanism of thymic atrophy is neither well defined nor well studied. Overall, the thymus shows an age-related loss of function and subsequent atrophy after puberty (Hartwig & Steinmann, 1994). Previous studies investigated methods of inducible thymus regrowth, or regeneration, through androgen restriction and gonadectomy (Brunelli et al., 1992; Hollander et al., 2010; Sutherland et al., 2005). Largely, these experiments found that thymocyte output is reconstituted and may indeed be greater in regenerated thymus. However, more recent data from Griffith et al. (2012) suggests that regenerated thymuses do not rescue the observable decrease in tissue-restricted antigen (TRAs) expression in post-castrated mice. Most importantly, TRAs are crucial to proper T cell development in self-tolerance. Even though castrations, androgen blockades and other supplementations experiments have shown mixed results, these

techniques have limiting scope of application because the effects of regeneration are transient (Griffith et al., 2012), these approaches are not equally applicable to both sexes, and are inconceivable in human studies. Consequently, researchers look towards other mechanisms to regenerate thymus function.

As previously discussed, thymocytes undergo rapid proliferative activity between DN1 and pre-DP stages. There is high anabolic metabolism within the thymus caused by proliferating lymphoid cells. Thus, the thymus is susceptible to high levels of stress and eventual wear. Likewise, age-related loss of function is observed across other organs such as heart, lung, and other tissues in general. This phenomenon is widely accepted in the scientific community and is attributed to the free radical theory of aging (Hartman, 1956). The theory postulates that over the course of an aerobic organism's life span, accumulated harmful byproducts of oxidative phosphorylation such as reactive oxygen species, or ROS, can lead to DNA damage and tissue degeneration (Hartman, 1956; Schriner et al., 2005). To counteract the degenerative effects of oxidative damage, the body naturally utilizes ROS scavenger enzymes such as superoxide dismutase (SOD), glutathione peroxidase (Gpx), peroxiredoxin (Prdx) and catalase (Cat) to alleviate DNA damage by reducing intra-tissue ROS levels. Several studies (Schriner et al., 2005; Wanagat et al., 2010) have evaluated how different scavengers, most notably catalase as a crucial terminal peroxide scavenger, systemically reduce DNA damage and may even contribute to an extension in lifespan when overexpressed in specific organisms. However, there has not been any conclusive study on the effects of catalase on thymus development.

Lastly, thymic stromal compartments provide a stable microenvironment for the transitory lymphocytes. Stromal cells provide the framework for the thymus as well as to secrete signal molecules to interact with transitory thymocytes. In addition, thymocytes may theoretically "leak" metabolic waste products in the stromal compartments (Hartman, 1956). These stromal cells are more susceptible to age associated changes from oxidative damage (Griffith et al., 2012). An earlier study from our research group (Griffith et al., 2009) established a differential gene expression mapping technique and generated microarray data that suggested the cortical compartment of the thymus was enriched in anabolic metabolism gene pathways relative to the medulla. Supplemental data from those gene enrichment experiments also showed expression of all previously mentioned peroxide scavengers in medullary and cortical lymphocytes and medullary stromal cells. But noticeably, there is no catalase expression in cortical stromal cells, as shown in the first two columns of Fig. 3. This data also suggested that mechanisms for DNA damage repair such as nucleotide excision repair, mismatch repair, or oxidation repair have lower expressions in cortical stromal cells. Therefore, with low activity of DNA repair mechanisms, the role of terminal peroxide scavengers such as catalase is doubly important.
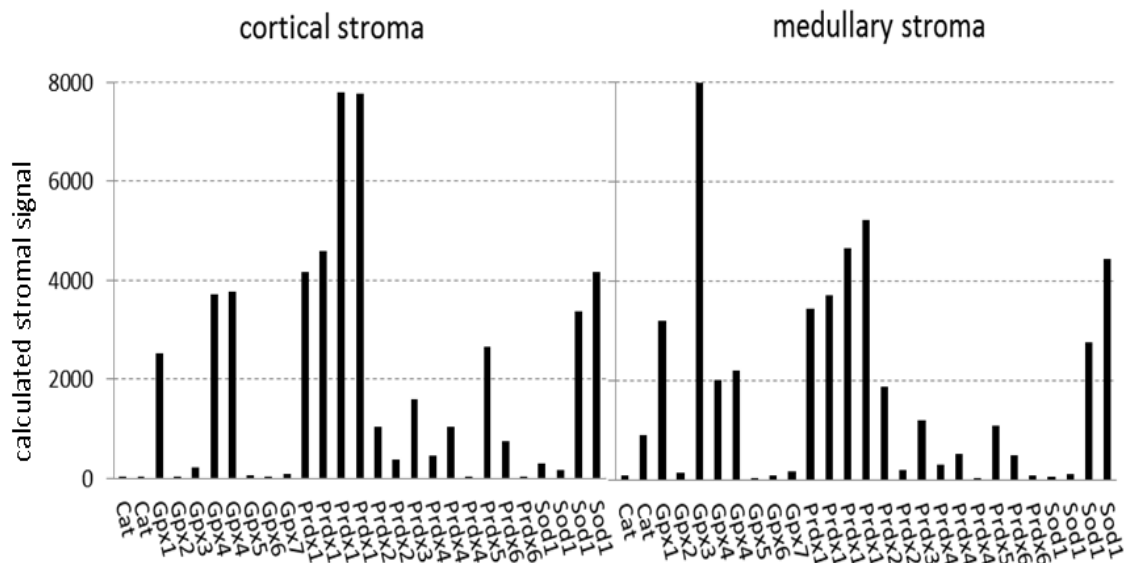
Figure 3. Peroxide scavengers in thymus. Gene enrichment data showing relative expression in cortical and medullary stroma. Each repeated gene class represents different gene probesets.

Since catalase is not highly expressed in mice stromal cells, we utilized a transgenic model overexpressing human catalase gene, targeted to the mitochondria (mCat). Over the years, catalase has been targeted to other cellular compartments including nucleus (nCat) and peroxisomes (pCat) (Schriner et al., 2005). We utilized a mCat transgenic mice model to target the mitochondria as a premiere contributor of free radicals in cells which may contribute to thymus atrophy. Throughout this study, we investigated if transgenic catalase influences T-cell development and affects the overall weight or size of the thymus. Our hypothesis is that thymic atrophy is caused largely by oxidative damage to vulnerable cortical stromal cells, and could therefore be prevented or mitigated by increasing catalase expression.

METHODS

The goal of this study was a straightforward comparison of various organ weights,

cellularity and histology for mCat$^{+/-}$, wildtype mice. In this case, mCat$^{+/-}$ are positive

transgenic models (Tg$^+$), while wildtype (WT) controls are negative controls.

Mice

For the purposes of this study, wildtype (WT) mice are standard C57BL/6 (B6)

background mice. We obtained mCat transgenic mice from Dr. Peter Rabinovitch

(University of Washington collaborator). Mice genotyping was confirmed using

established procedures. Mice at various ages were used in accordance to procedures

approved by the Scripps-Florida Institutional Animal Care and Use Committee.

Preliminary Test: Antioxidant Dietary Supplementation

In order to test our predictions about the role of reactive oxidative species and thymic

atrophy, we designed a simple experiment to supplement the drinking water of young

weanling mice with known antioxidants. These young mice received vitamin C (vitC, 5

mg/ml), or N-acetyl cysteine (NAC, 40 mM) for 7 weeks of supplementation. Control

mice cohorts did not receive antioxidant supplementation. Therefore, at ten weeks of age

all mice were assessed: whole organs weights for kidney, liver, heart, and spleen as well

as body composition were measured. We chose a ten week assessment point because

thymus size in WT mice shows steady atrophy at 60% of the previous 4-5 week peak

size.

Tissue Extraction and Cell Suspension

Transgenic and wildtype mice were euthanized using carbon dioxide and cervical

dislocation was performed. The animal's mass was recorded using a top loading balance.

All steps were performed at 4°C. Whole organs such as thymuses, kidneys, hearts and

spleens were collected and stored in ice-cold MTH medium (Hank's balanced salt

solution) containing 95% MTH, 5% FBS and 0.5% DNAse. Organ masses were

measured using analytical balance. Next, single cell suspension samples were prepared

from whole thymuses by passage through a cell strainer.

Cell Purification and Flow Cytometry

Single-cell suspensions from thymuses were counted using a hemacytometer utilizing

eosin exclusion as a viability dye. Cell suspensions were then labeled with a cocktail of

rat antibodies (Abs) recognizing various lineage markers (CD3, CD4, CD8, CD19, Mac-

1, Gr1, Nx1, Thy1, B220, and mAB Ter 119 (erythrocyte marker)), and subsequently

stained with Red-613 anti-rat Ig (Caltag Laboratories). In addition, cells were stained

with commercial Ab conjugates for c-Kit (ACK-2, biotin conjugate, followed by

streptavidin-Alexa Fluor 660) and CD25-PE. In a separate analysis, thymocytes were

stained with commercial Ab conjugates for CD4-E and CD8-APC. Labeled samples were

analyzed on a BD LSRII flow cytometer. Sort gates were customized to count lineage

negative (lin⁻) cells as wells as singlet thymocyte populations. Dead cells were excluded

using DAPI (4',6'-diamidino-2-phenylindole, 0.1 µg/ml). Viable thymocytes were

analyzed using FlowJo software (Tree Star) and were gated based on forward and side scatter properties. (Umland2007; Chen2008; Griffith, et al., 2009).

Tissue Sectioning and Immunofluorescence Staining

One thymus lobe, as well as additional intact tissues of kidney and spleen were collected and immediately frozen in O.C.T compound (Tissue-Tek). Frozen tissues were sectioned on a cryostat into 8-20μm transverse slices and mounted on glass slides. Slide-mounted tissue sections were fixed in cold acetone, dried at room temperature, and then rehydrated with PBS/5% FBS. Following subsequent washes with PBS/FBS medium, tissue was stained with antibody cocktails containing FITC-conjugated, anti-pan keratin, and directly conjugated catalase-Alexa 594 antibodies. Slides were mounted and coverslipped using Prolong mounting media (Introvogen) with DAPI (as a nuclear marker; 1:200 dilution). Fluorescent images were captured using a BX51 microscope (Olympus) equipped with a charge-coupled device (CCD) camera mount and CellSens software.

RESULTS

The aim of our experiment was to investigate how overexpression of transgenic catalase affects T-cell development in the thymus. Gene expression studies have shown that stromal cells express low levels of catalase, a terminal peroxide scavenger of reactive oxygen species. Given that the thymus atrophies relatively early in life, we predicted that the lack of catalase in cortical cells could result in increased oxidative damage in those cells and eventually in thymic atrophy. To test this hypothesis, we used a transgenic model to over-express catalase in all cells, including cortical stroma and evaluated the effect on thymus size and T-cell development.

Preliminary Antioxidant Supplementation Results

All groups of mice were assessed at 10 weeks of age after 7 weeks of supplementation. During the treatment, the mice were active and well groomed, and increased their body weight (Table 1). Control group mice received normal drinking water while their cohorts received drinking water with 2.6g/kg ascorbate (Vit. C) or 2.7g/kg N-acetyl cysteine (NAC). These values for our estimated daily dose were the higher than recommended daily allowances of 0.0007g/kg and 1.9g/kg for ascorbate and NAC respectively. Nevertheless, dosages used for our studies were maximum therapeutic doses that had been reported in previous scientific literature. Body composition was measured by MRI, and the organ weights were recorded after treatment. There were no significant increases in body weights for either NAC or Vit. C treated mice. Nevertheless, substantial differences in organ weights were observed in thymus in contrast to other

14

organs. Both NAC (p< 0.001) and Vit. C (p<0.002) groups had significantly larger

thymuses when compared to control; averaged normalized values for organ weight to

body weights (mg/g) are shown in Fig. 4. Furthermore, NAC-treated group had

comparative thymic masses to younger 4-5 week old mouse (recorded peak size from

previous studies before atrophy).

Table 1. Body weights (in grams) pre and post dietary antioxidant supplementation. Averages shown with standard deviations

Id No.	NAC		Ascorbate		Control	
	pre	post	pre	post	pre	post
1	12.8	19.4	12.6	17.6	14.4	25.8
2	12.4	23.6	14	20.4	13.6	28.4
3	14.1	18.1	14.5	23.8	14.8	29.7
4	14.3	18.9	11.7	19.7	11.2	31
5	12.5	21.2	14.9	20.1	15.5	24.1
Averages	13.2±0.9	20.2 ± 2.2	13.5 ± 1.3	20.3 ±2.2	13.9 ± 1.7	27.8±2.8
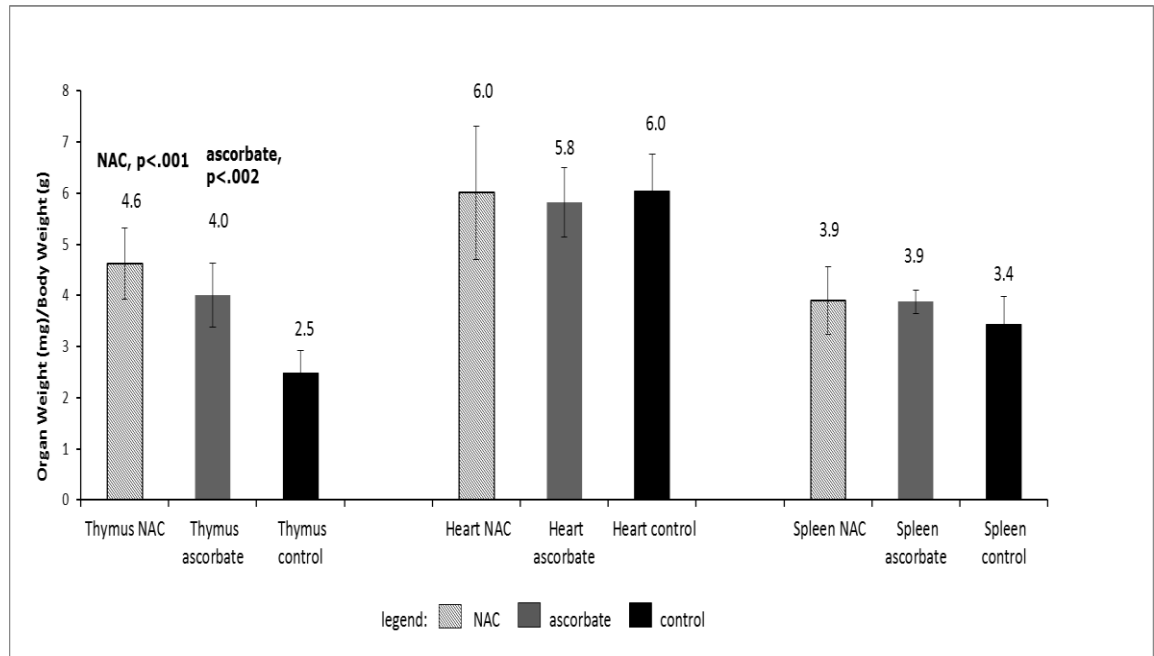
Figure 4. Organ weight normalized to body weight (mg/g). The average relative weights of organs were normalized to the body weights for all mice groups. Mean ± S.D. for groups are shown. Differences were calculated using two-tailed Student's t-test. Significant differences were found only in the thymus (NAC, p<0.001; ascorbate, p<0.002).

15

Thymocyte Peroxidase Gene Expression Results

In Fig. 3 (previously shown), we observed that catalase expression was low in stromal cells; however, catalase was present in medullary stromal cells as well as lymphoid cells. Since catalase is expressed in these transitory lymphoid cells (DN1 to SP stages), we investigated when catalase expression is upregulated or downregulated during thymocyte development. We utilized a differential gene expression mapping technique to quantify gene expression during different stages of development. We found that catalase expression steadily increases from double negative (DN) stages and peaks at the small double positive (DP) sub-stage (Fig. 5). After catalase expression peaks, its expression sharply declines as thymocytes enter single positive (SP) stages. To clarify, SP stages are represented in Fig. 5 as separate CD4 and CD8 stages. In contrast to catalase expression, we observed that Glutathione peroxidase, another ROS scavenger, exhibits an inverse trend to catalase expression, starting with an overall decline between DN1 and preDP stages and drastically falls during the blast DP stage, and then slightly increases toward at the SP stages. It is important to note that scavenger levels shown in Fig. 5 are normalized values and are otherwise very high (several times the chip median (500)) at all stages in lymphocytes. Therefore, lymphocytes appear to be well protected from ROS.
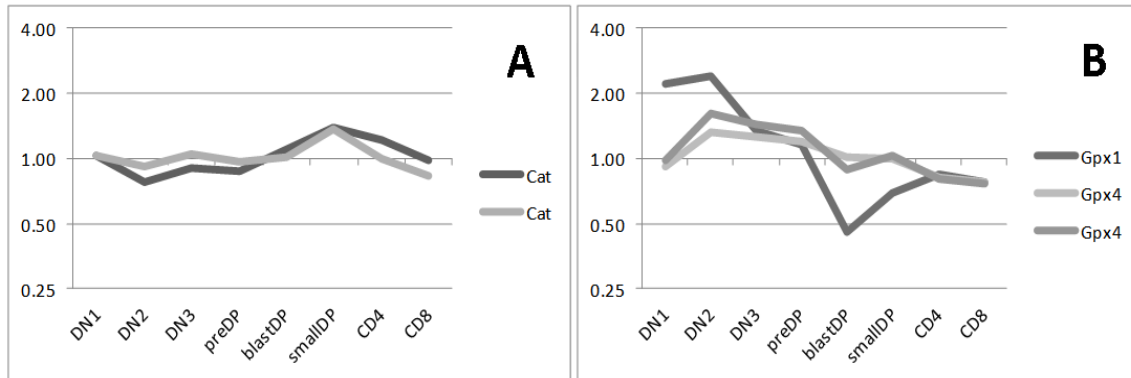
Figure 5. Comparison of lymphocyte gene expression for Catalase (Cat) and Glutathione peroxidase (Gpx). Normalized values shown for gene expressions. Each line on the graph represents a different gene probe set. (A) Catalase expressions showing increasing trend and then peak at small DP stage then sharp decrease. (B) Glutathione peroxidase expression with overall decreasing trend.

mCat Results

We expected that expression of transgenic catalase targeted to the mitochondria would influence the body and organ weights of Tg$^+$ mice when compared to WT mice. However, the most significant increases were observed in thymus cellularity of mCat mice.

Body and Organ Weights:

All animals were evaluated at 14 weeks of age. Discrepancies in sample size between wildtype and Tg mice are due to availability of mice when experiment was conducted. From the body and organ weight data listed below in Fig. 6, we found that for all samples (males and females), there were no significant differences in mCat animal weights when compared to wildtype control.
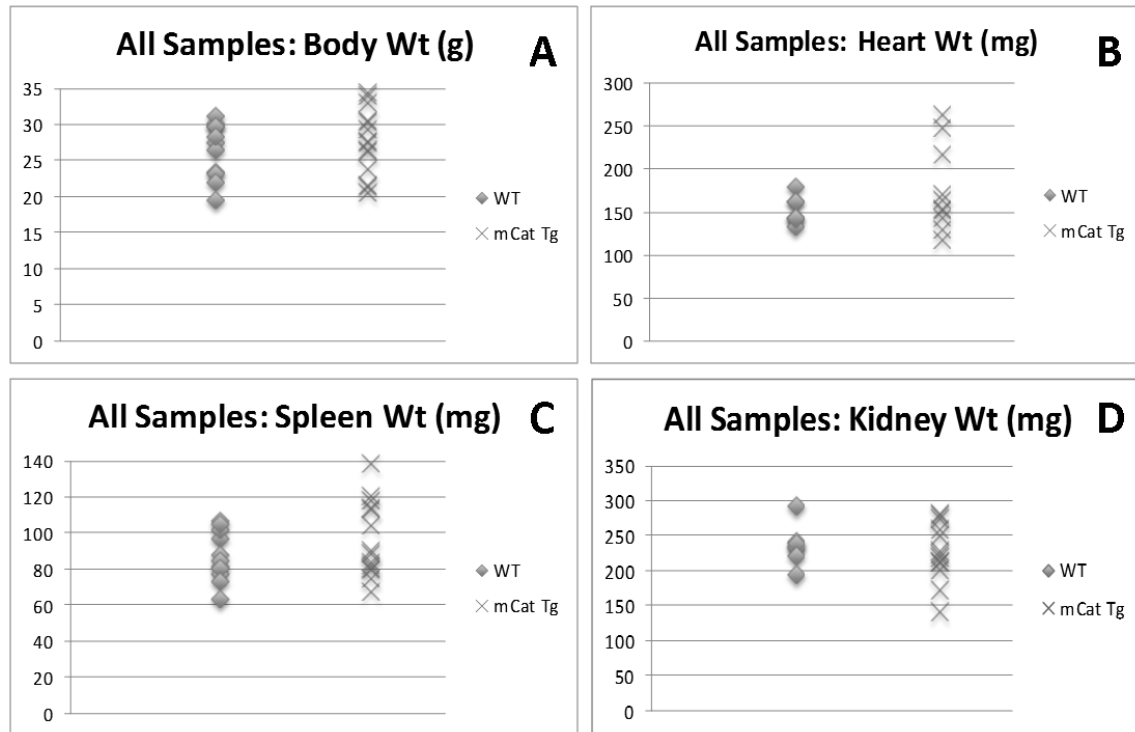
Figure 6. Distribution of body and organ weights. Figures 5A-D shows the measured masses of whole organs (kidney, spleen, and heart) and mice body weights. All samples represent both male and females animals sampled. There were no observed differences across all organ and body weights when compared to control. (A) n=11 WT; n=12 mCat Tg. (B) n=7 WT; n=10 mCat Tg. (C) n=12 WT; n=14 mCat Tg. (D) n=7 WT; n=13 mCat Tg.

On the other hand, thymus cell numbers showed statistically significant differences among males ($p<0.007$) and females ($p<0.00007$), and an overall change in thymus cellularity for all samples ($p<0.00004$) (shown in Fig. 7). Directly counting thymus cells provides a better measurement of thymic mass and reduces discrepancies in techniques for weighing whole thymuses. Total cell numbers (in millions) were calculated by doubling the cell numbers obtained from one harvested lobe.

Figure 7. Thymus cell numbers (in millions). Cell numbers are from 1 lobe, multiplied by 2. Statistically significant changes in cellularity were observed in thymuses of both male and female mice. Differences between groups were calculated using two-tailed t-test. (A) p<0.007 between WT and mCat Tg males. (B) p<0.00007 between WT and mCat Tg females. (C) p<0.00004 between all WT and mCat Tg samples; n=13 and n=22, respectively.

Thymocyte Phenotype:

An evaluation of the thymocyte phenotypes was performed using flow cytometry to determine the percentages of the thymocytes at various stages of development (DN or SP subsets and lineage negative (lin-) cells). Overall, we found no significant differences in subset numbers or percentages (Fig. 8). Thymocyte subset percentages of mCat mice were relatively equal to WT (Fig. 8A). Likewise, lineage negative cells (all progenitor cells that have not committed to CD4/CD8 lineages) did not show any significant trends (Fig. 8B). Nevertheless, we observed an increase in thymocyte numbers for mCat mice during the DN and DP stages (Fig. 8C). Further analysis of the DN subsets showed an overall increasing trend between the DN3 and preDP transition (Fig. 8D).

19
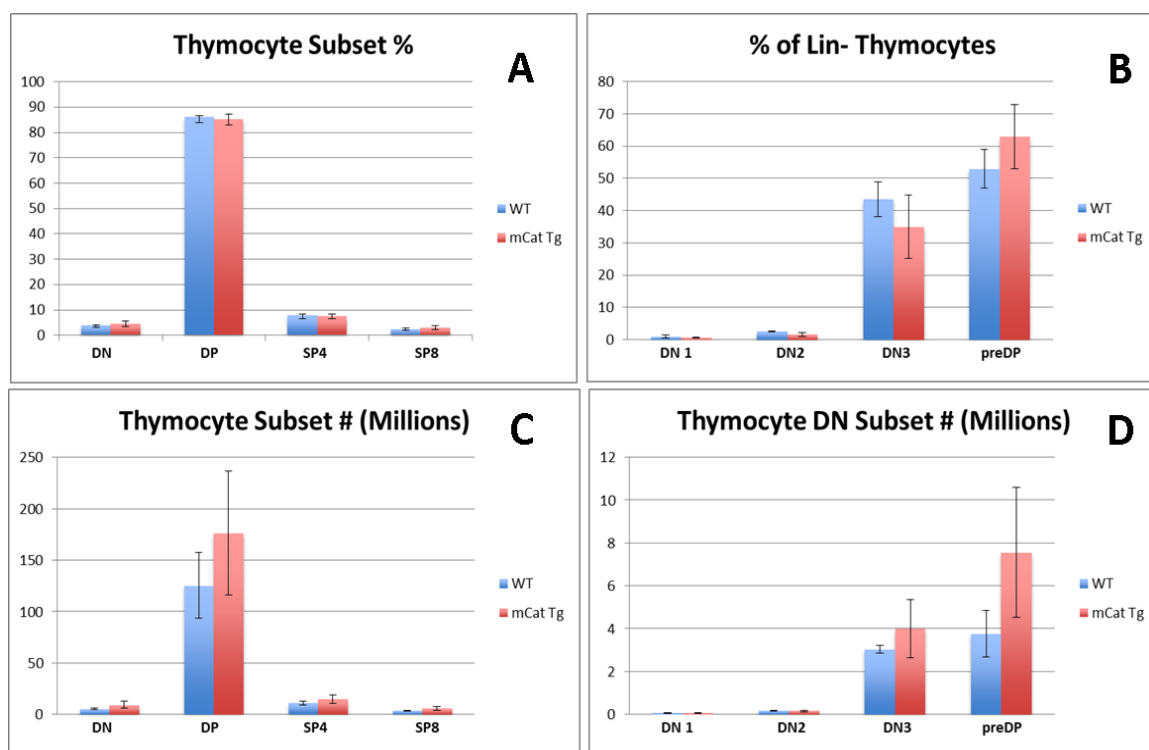
Figure 8. Thymocyte subset numbers and percentages. Overall, there were no significant differences between mCat Tg and WT mice.

Immunofluorescence (IF) Staining:

Next, we detected the presence of endogenous catalase in stromal cells of frozen thymus sections from WT mice. Antibody (Abs) staining was performed using FITC-conjugated anti-pan keratin and AlexaFluor-594-conjugated anti-catalase. Anti-pan keratin provides a cytoskeleton stain and marks all epithelial stromal cells in green. Stromal cells in the cortex are characterized by stellate shape while those in the medulla usually have a reticular morphology. In Fig. 9, cells expressing catalase are marked in red. Cells co-expressing catalase and pan-keratin appear yellow. We observed that the catalase expressing cells in the cortex were all keratin negative, the majority of which are

lymphocytes, indicating that catalase expression did not occur in epithelial cells, consistent with our microarray results. However, in the medulla, catalase-expressing cells are observed in both epithelial cells (yellow stain resulting from keratin-catalase co-localization) and in non-epithelial cells (mostly lymphocytes). We observed the greatest number of cells co-expressing catalase and pan-keratin at the medullary side of the cortico-medullary junction.
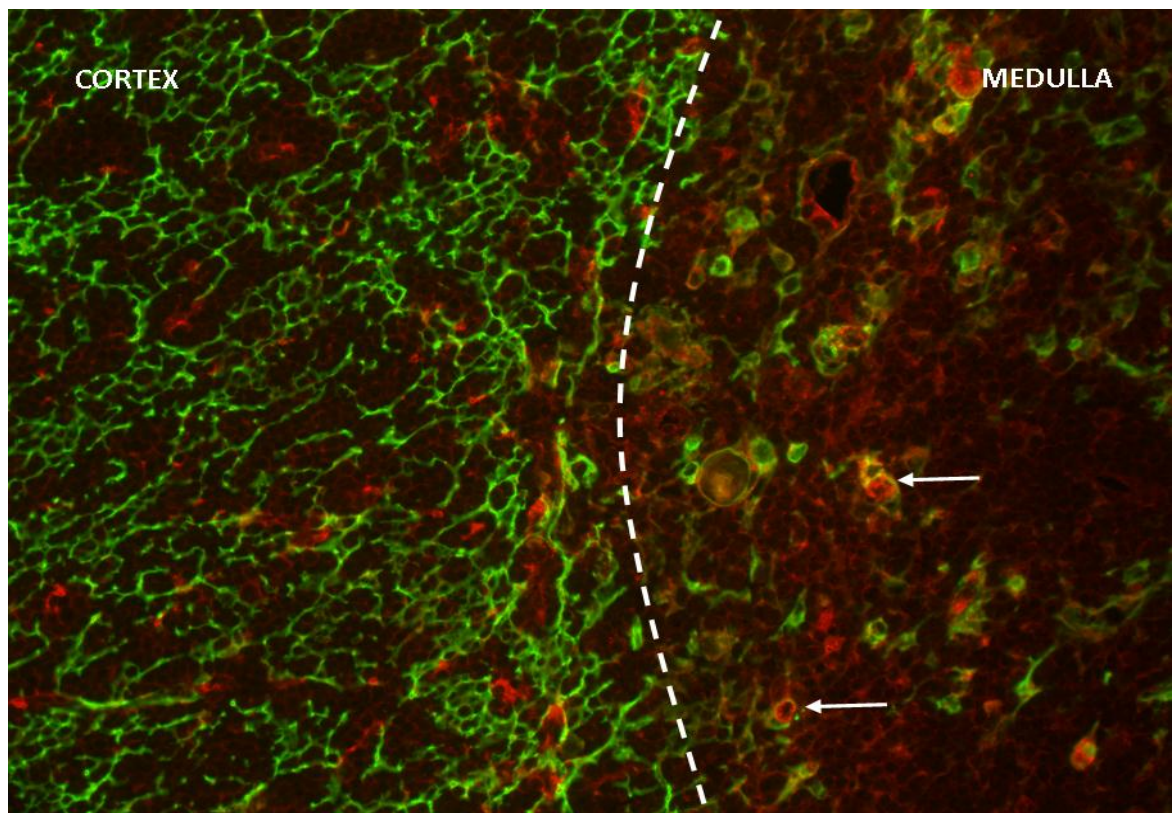
Figure 9. Catalase stain in frozen thymus section. 20x magnification**.** Anti-pan keratin in epithelial cells (green); cells expressing catalase (red). Arrows denote examples of stromal cells co-expressing catalase and pan-keratin (yellow).

DISCUSSION

I investigated the role of transgenic human catalase (targeted to the mitochondria, mCat) in T cell differentiation and thymus development of heterozygous mice. More specifically, our work analyzed how the overexpression of the transgene in the cortical stromal regions may mitigate thymic atrophy. We worked under the assumption that highly metabolic lymphoid cells leaked harmful oxidative byproducts or reactive oxygen species, ROS, into the stromal compartments that led to further degradation of the stromal integrity. Furthermore, our previous data showed a lack of DNA repair enzymes and relatively low catalase expression in cortical stromal cells (Griffith et al., 2009). We hypothesized that low catalase expression coupled with DNA repair deficiencies made the cortical stromal cells particularly vulnerable to oxidative stress, and eventually contributed to rapid thymic atrophy. To test this hypothesis, we obtained a constitutively active transgenic mouse model to increase catalase expression and analyzed how the body weights, whole organ weights, thymus cellularity, and T-cell differentiation changed between transgenic and wildtype (WT) mice.

In particular, we found the following. First, the average body weight for mCat animals increased slightly; however, there were no significant differences between WT and mCat mice. This finding is consistent with previous literature (Schriner et al., 2005) that suggested that transgenic mice did not have differences in weight or any physical abnormalities. Likewise, the weights for spleen, kidney and heart were not statistically different between animal groups.

22

Second, from our analysis of thymus single cell suspensions, we found that total thymus cellularity increased in mCat mice. There was a marked statistical difference in thymic cellularity for all samples (P<0.00004) of transgenic animals when compared to WT. This significant difference was also exemplified between male and female mCat mice. In general, we observe that female mice are usually physically smaller (and have lower average body weights) than their male cohorts. Nevertheless, females had larger thymuses on average in both WT and mCat mice. We observed that the difference in total cell numbers for female transgenic mice was highly significant (P<0.00007). Male transgenic mice also showed statistical differences in thymus cellularity when compared to WT (P<0.007).

In further analysis, we evaluated progression of thymocytes through the major developmental stages (double negative (DN), double positive (DP), and single positive (SP)) and did not observe any significant differences between mCat and WT animals. Thymocyte percentages throughout these sub-stages were similar in mCat and WT mice (as shown in Fig. 8A). Lineage negative thymocytes, which have not committed to T-cell lineages and could potentially adopt other lineages outside of the thymic environment, showed no significant differences (Fig. 8B).

Thus, we observe a change in thymic cellularity without changing T-cell development. Since the total cellularity depend on the health of both stromal and lymphoid compartments, and since the stromal but now lymphoid cells were catalase deficient in WT mice, we may further hypothesize that stromal cells received the most noticeable benefits of catalase overexpression - that is, less degradation of stromal

integrity by reactive oxygen species (ROS) and subsequent increase in stromal cell numbers. Therefore, we would expect decreased ROS levels in transgenic animals and a subsequent decrease in thymic atrophy. In order to test the ability of our mCat mice in protecting against ROS-induced damages, we plan to detect and quantify ROS levels abd DNA damage in thymic tissue, in particular stromal cells.

Our central hypothesis for this research is that longer-lived, catalase deficient stromal cells are more susceptible to ROS-induced damages than transient lymphocytes (which also have shown efficient protection with higher expressions of peroxide scavenger enzymes and repair genes). For future studies, we plan to test for and quantify DNA damage in-situ and/or ex-vivo. We primarily plan to test this using immunohistochemistry and immunofluorescence. DNA damage may be measured by quantifying the presence of 8-oxo-dihydro-2'-deoxyguanosine (8-oxo-dG) which results from ROS-induced base oxidation of DNA nucleotides. Earlier this year, we began testing anti-8-oxo-dG monoclonal antibody (clone 2E2, Trevigen); however, we were unable to detect significant immunofluorescent expression in snap-frozen thymus tissue. More recently, we have looked into other reagents that may quantify DNA damage for both lymphoid and stromal cells ex-vivo and in-situ, including the comet assay. Comet assay kits (Trevigen) are commercially available and allow for an assessment of DNA damage. From these experiments, we expect that stromal cells from mCat animals will have increased prevention of DNA damage when compared to WT mice with low levels of endogenous catalase. This kit can also be used to assess DNA repair in cells incubated overnight after DNA damage induced experimentally by hydrogen peroxide.

24

In summary, results from our studies with catalase transgenic animals support the notion that increased protection against oxidative damage can diminish thymic atrophy without altering T-cell development. Future studies will address the mechanisms by which catalase expression protects thymus tissue.

APPENDIX:

RAW DATA

A. Peroxide Scavenger Gene Expression

Gene Symbol	Probe Set ID	Entrez Gene	Y CS	Y MS
Cat	1416430_at	12359	0.01	94.76
Cat	1416429_a_at	12359	0.01	902.76
Gpx1	1460671_at	14775	2517.8	3199
Gpx2	1449279_at	14776	17.09	139.82
Gpx3	1449106_at	14778	226.12	12682
Gpx4	1451695_a_at	625249	3729.2	2007.1
Gpx4	1456193_x_at	625249	3762.2	2215.8
Gpx5	1420698_at	14780	58.61	30.79
Gpx6	1452135_at	75512	25.04	85.1
Gpx7	1417836_at	67305	87.61	164.25
Prdx1	1416000_a_at	18477	4159.9	3439.2
Prdx1	1433866_x_at	18477	4584.5	3721
Prdx1	1434731_x_at	18477	7793	4658
Prdx1	1436691_x_at	18477	7770.5	5246.2
Prdx2	1418506_a_at	21672	1055.3	1874.3
Prdx2	1430979_a_at	21672	381.64	196.53
Prdx3	1416292_at	11757	1600.3	1196.2
Prdx4	1416166_a_at	53381	453.37	322.01
Prdx4	1416167_at	53381	1038.4	524.83
Prdx4	1431269_at	53381	23.43	34.26
Prdx5	1416381_a_at	54683	2663.6	1086.4
Prdx6	1423223_a_at	11758	745.49	486.35
Prdx6	1442878_at	11758	15.54	97.7
Sod1	1435304_at	20655	298.5	65.72
Sod1	1440222_at	20655	180.91	132.78
Sod1	1451124_at	20655	3377.5	2765.4
Sod1	1459976_s_at	20655	4170.5	4445.1

Y CS – cortical stroma, young mice

Y MS – medullary stroma, young mice

B. Antioxidant Preliminary Experiment:
    i. Standard weights for antioxidant supplemented mice

	Body weight (g)			Thymus wt (mg)		
	NAC	ascorbate	control	NAC	ascorbate	control
mouse 1	19.4	17.6	25.8	101.2	76	65.1
mouse 2	23.6	20.4	28.4	86.8	75.7	63
mouse 3	18.1	23.8	29.7	96.8	76.9	69.1
mouse 4	18.9	19.7	31	79.1	95.8	66
mouse 5	21.2	20.1	24.1	99.3	78.4	77.7
Average	**20.24**	**20.32**	**27.8**	**92.64**	**80.56**	**68.18**
Standard deviation	2.19613	2.23316	2.824	9.38579	8.58388	5.75647
T-test to control	0.001492	0.001654		0.001097	0.027994	

	Kidney wt (mg)			Heart wt (mg)		
	NAC	ascorbate	control	NAC	ascorbate	control
mouse 1	352.6	302	445.6	113.1	97.1	141.3
mouse 2	324.6	331	509	94.8	108	172.7
mouse 3	447.1	446.9	472.1	137.4	160.8	183.2
mouse 4	387.2	348.8	428.5	116.2	103.2	164.3
mouse 5	379.6	364.8	508.3	136.6	127.3	172.1
Average	**378.22**	**358.7**	**472.7**	**119.62**	**119.28**	**166.72**
Standard deviation	45.7124	54.5359	36.3093	17.8514	25.8166	15.7188
T-test to control	0.00054	0.001292		0.00054	0.001292	

	Spleen wt (mg)		
	NAC	ascorbate	control
mouse 1	74.6	70.7	78.9
mouse 2	74.2	75.7	102.9
mouse 3	87.4	84.6	115.1
mouse 4	65.3	81.1	83.3
mouse 5	89.6	80.1	95.2
Average	**78.22**	**78.44**	**95.08**
Standard deviation	10.1238	5.36638	14.6844
T-test to control	0.00054	0.001292	

ii. Normalized weights for antioxidant expressions

	thymus (mg) / body weight (g)			heart (mg) / body weight (g)		
	NAC	ascorbate	control	NAC	ascorbate	control
mouse 1	5.216495	4.318182	2.523256	5.829897	5.517045	5.476744
mouse 2	3.677966	3.710784	2.21831	4.016949	5.294118	6.080986
mouse 3	5.348066	3.231092	2.326599	7.59116	6.756303	6.16835
mouse 4	4.185185	4.862944	2.129032	6.148148	5.238579	5.3
mouse 5	4.683962	3.900498	3.224066	6.443396	6.333333	7.141079
Average	**4.6223**	**4.0047**	**2.4843**	**6.0059**	**5.8279**	**6.0334**
Standard deviation	0.70115	0.61858	0.43892	1.29534	0.67938	0.72374
T-test to control	0.000415	0.002049		0.967934	0.65567	

	spleen (mg) / body weight (g)		
	NAC	ascorbate	control
mouse 1	3.845361	4.017045	3.05814
mouse 2	3.144068	3.710784	3.623239
mouse 3	4.828729	3.554622	3.875421
mouse 4	3.455026	4.116751	2.687097
mouse 5	4.226415	3.985075	3.950207
Average	**3.8999**	**3.8769**	**3.4388**
Standard deviation	0.65983	0.2347	0.54684
T-test to control	0.263324	0.138391	

C. Lymphocyte gene expressions for Cat and Gpx

Measured Values (MAS5)

symbol	DN1	DN2	DN3	preDP	blastDP	smallDP	CD4	CD8	probeset ID
Cat	1592	1196	1393	1353	1713	2135	1885	1508	1416429_a_at
Cat	3175	2812	3192	2933	3083	4151	3035	2522	1416430_at
Gpx1	19678	21545	11965	10291	4104	6220	7587	6949	1460671_at
Gpx4	6139	8892	8455	8003	6777	6692	5522	5226	1451695_a_at
Gpx4	5188	8635	7721	7134	4711	5482	4306	4082	1456193_x_at

Normalized values

	DN1	DN2	DN3	preDP	blastDP	smallDP	CD4	CD8
Cat	1.03	0.77	0.90	0.87	1.11	1.38	1.22	0.97
Cat	1.04	0.92	1.04	0.96	1.01	1.36	0.99	0.82
Gpx1	2.20	2.41	1.34	1.15	0.46	0.70	0.85	0.78
Gpx4	0.91	1.32	1.26	1.19	1.01	0.99	0.82	0.78
Gpx4	0.97	1.62	1.45	1.34	0.88	1.03	0.81	0.77

D. mCat Thymocyte Subset Phenotypes
   i.   Thymocytes Percentages

Mouse ID	Genotype	%DN	%DP	%SP4	%SP8
36	Tg	3.63	86.7	7.06	2.62
37	Tg	4.12	86.1	6.93	2.81
38	Tg	5.36	82.1	9	3.59
39	Tg	4.44	84.6	8.25	2.75
41	Tg	6.6	82.5	6.85	4.04
42	Tg	4.16	85.4	7.45	2.99
49	Tg	3.6	88.3	6.6	1.52
	Avg	4.559	85.100	7.449	2.903
	Standard deviation	1.07673	2.232338	0.870583	0.795523
40	WT	5	82.9	8.83	3.28
43	WT	3.8	85.1	8.51	2.61
45	WT	3.37	88.1	6.59	1.94
46	WT	3.19	88.2	6.6	1.98
47	WT	3.55	85.5	8.2	2.71
	Avg	3.782	85.960	7.746	2.504
	T-test	0.19	0.53	0.61	0.36
	Standard deviation	0.717266	2.231143	1.074072	0.558686

ii. Thymocyte # (Millions)

Mouse ID	Genotype	%DN	#DN	#DP	#SP4	#SP8
36	Tg	3.63	5.425529	129.585	10.55213	3.915947
37	Tg	4.12	7.058957	147.5185	11.87344	4.814483
38	Tg	5.36	8.61829	132.0078	14.47101	5.772325
39	Tg	4.44	6.531851	124.4582	12.13688	4.045628
41	Tg	6.6	14.45661	180.7077	15.00421	8.849199
42	Tg	4.16	11.91208	244.5413	21.33293	8.561808
49	Tg	3.6	11.15977	273.7243	20.45958	4.711903
	Avg	**4.559**	**9.309**	**176.078**	**15.119**	**5.810**
	Standard deviation	1.07673	3.292238	60.31514	4.239708	2.06994
40	WT	5	5.935951	98.41807	10.48289	3.893984
43	WT	3.8	5.705247	127.7675	12.77675	3.918604
45	WT	3.37	4.161907	108.8024	8.138565	2.395875
46	WT	3.19	6.482779	179.2417	13.41265	4.023794
47	WT	3.55	4.693194	113.0333	10.84062	3.582692
	Avg	**3.782**	**5.396**	**125.453**	**11.130**	**3.563**
	T-test	0.19	0.03	0.12	0.08	0.04
	Standard deviation	0.717266	0.94673	31.86285	2.084073	0.672849

iii. Lineage negative Percentages

Mouse ID	Genotype	%DN1	%DN2	%DN3
36	Tg	0.76	1.8	47.2
37	Tg	0.8	2.16	37.6
38	Tg	0.44	1.25	19.1
39	Tg	0.75	1.88	29.7
41	Tg	0.41	0.67	41.7
42	Tg	0.69	1.38	34
	Avg	**0.642**	**1.523**	**34.883**
	Standard deviation	0.171746	0.535263	9.82149
40	WT	1.26	2.67	47.4
43	WT	0.7	2.36	39.8
	Avg	**0.980**	**2.515**	**43.600**
	T-test	0.12	0.05	0.29
	Standard deviation	0.39598	0.219203	5.374012

iv. Thymocyte DN subsets # (Millions)

Mouse ID	Genotype	#DN1	#DN2	#DN3	#preDP
36	Tg	0.068269	0.16169	4.239864	4.509347
37	Tg	0.067574	0.18245	3.175982	5.025823
38	Tg	0.069332	0.196967	3.009648	12.4798
39	Tg	0.064656	0.162072	2.560397	5.836326
41	Tg	0.060799	0.099354	6.183685	8.482177
42	Tg	0.097605	0.195209	4.809502	9.039035
	Avg	**0.071**	**0.166**	**3.997**	**7.562**
	Standard deviation	0.013216	0.036216	1.35746	3.031235
40	WT	0.077785	0.164829	2.926187	3.006441
43	WT	0.055596	0.187438	3.161037	4.542998
	Avg	**0.067**	**0.176**	**3.044**	**3.775**
	T-test	0.69	0.73	0.38	0.15
	Standard deviation	0.01569	0.015987	0.166064	1.08651

E. mCat body and organ weights at 14 weeks

All Samples: Body Wt (g)		All Samples: Spleen Wt (mg)	
WT	Tg	WT	Tg
27.5	30.6	97.16	104.21
30.3	33	107.15	113.77
23.4	27.6	81.66	118.38
26.5	23.9	101.92	120.58
29.8	34.6	87.92	138.54
31.2	30.5	105.24	90.53
29.8	34.1	77.63	114.68
23.3	26.3	84.66	74.7
28.4	27.7	81.04	82.34
22.1	29.4	73.77	88.85
19.6	26.6	63.85	80.1
	21.4		84.2
	20.7		67.64
	21.7		80.36
n=11	n=12	n=12	n=14

31

All Samples: Kidney Wt (mg)

WT	Tg
292.39	281.62
241.89	251.27
195.7	213.29
232.5	201.35
235.18	280.25
239.81	259.5
221.38	275.52
	213.6
	223.64
	228.02
	220.87
	173.43
	141.11
n=7	n=13

All Samples: Heart Wt (mg)

WT	Tg
162.47	218.22
179.76	264.11
144.6	248.77
133.58	171.4
163.2	152.2
141.52	165.2
143.53	154.4
	130.15
	117.7
	143.49
n=7	n=10

All Samples: Thymus Cell # (Millions)

WT	Tg
204	284
176	292
166	372
136	360
238	520
138	468
234	536
180	286
230	172
306	358
163	370
251	252
170	422
	245
	230
	276
	250
	232
	356
	410
	298
	390
n=13	n=22

Thymus Cell # (Millions)

Females

WT	Tg
136	360
238	520
230	468
251	536
170	358
	370
	356
	410
	390
n=5	n=9

Thymus Cell # (Millions)

Males

WT	Tg
204	284
176	292
166	372
138	286
234	172
180	252
306	422
163	245
	230
	276
	250
	232
	298
n=8	n=13

REFERENCES

Brunelli, R., Frasca, D., Spano, M., Zichella, L., & Doria, G. (1992). Gonadectomy in old

    mice induces thymus regeneration but does not recover mitotic responsiveness.

    Annals of the New York Academy of Sciences, *673*, 252-255.

Cruse, J. M., & Lewis, R. E. (1999). *Atlas of immunology.* Boca Raton, FL: CRC Press.

Griffith, A. V., Fallahi, M., Nakase, H., Gosink, M., Young, B., & Petrie, H. T. (2009).

    Spatial mapping of thymic stromal microenvironments reveals unique features

    influencing T lymphoid differentiation. *Immunity*, *31*(6), 999-1009.

Griffith, A. V., Fallahi, M., Venables, T., & Petrie, H. T. (2012). Persistent degenerative

    changes in thymic organ function revealed by an inducible model of organ regrowth.

    Aging cell, *11*(1), 169-177.

Hartman, D. (1956). Aging: a theory based on free radical and radiation chemistry.

    Journal of gerontology, *11*(3), 298-300.

Hartwig, M., & Steinmann, G. (1994). On a causal mechanism of chronic thymic

    involution in man. *Mechanisms of ageing and development*, *75*(2), 151-6.

Haynes, B. F., Sempowski, G. D., Wells, A. F., & Hale, L. P. (2000). The human thymus

    during aging. *Immunologic research*, *22*(2-3), 253-61.

Hollander, G. A., Krenger, W., & Blazar, B. R. (2010). Emerging strategies to boost

    thymic function. *Current opinion in pharmacology*, *10*(4), 443-453.

Janeway, C. (1999). *Immunobiology: the immune system in health and disease*. (P.

    Travers, M. Walport, & D. J. Capra, Eds.) (4th ed., p. 635). New York: Current

    Biology Publications.

Kuby, J. (1997). *Immunology*. W.H. Freeman.

Petrie, H.T., & Zuniga-Pflucker, J. C. (2007). Zoned out: functional mapping of stromal signaling microenvironments in the thymus. *Annual Review of Immunology*, *25*, 649-679.

Petrie, H.T. (2002). Role of thymic organ structure and stromal composition in steady-state postnatal T-cell production. *Immunological reviews*, *189*, 8-19.

Prockop, S. E., Palencia, S., Ryan, C. M., Gordon, K., Gray, D., & Petrie, H. T. (2002). Stromal cells provide the matrix for migration of early lymphoid progenitors through the thymic cortex. *Journal of immunology (Baltimore, Md. : 1950)*, *169*(8), 4354-61.

Schriner, S. E., Linford, N. J., Martin, G. M., Treuting, P., Ogburn, C. E., Emond, M., Coskun, P. E., et al. (2005). Extension of murine life span by overexpression of catalase targeted to mitochondria. *Science (New York, N.Y.)*, *308*(5730), 1909-11.

Sutherland, J. S., Goldberg, G. L., Hammett, M. V., Uldrich, A. P., Berzins, S. P., Heng, T. S., Blazar, B. R., et al. (2005). Activation of thymic regeneration in mice and humans following androgen blockade. *Journal of immunology (Baltimore, MD: 1950)*, *175*(4), 2741-2753.

Wanagat, J., Dai, D.-F., & Rabinovitch, P. (2010). Mitochondrial oxidative stress and mammalian healthspan. *Mitochondria in Ageing*, *131*(7–8), 527-535.